Hydraulic transient wave separation algorithm using a dual-sensor with applications to pipeline condition assessment

He Shi, Jinzhe Gong, Aaron C. Zecchin, Martin F. Lambert and Angus R. Simpson

ABSTRACT

Over the past two decades, techniques have been developed for pipeline leak detection and condition assessment using hydraulic transient waves (i.e. water hammer waves). A common measurement strategy for applications involves analysis of signals from a single pressure sensor located at each measurement site. The measured pressure trace from a single sensor is a superposition of reflections coming from upstream, and downstream, of the sensor. This superposition brings complexities for signal processing applications for fault detection analysis. This paper presents a wave separation algorithm, accounting for transmission dynamics, which enables the extraction of directional travelling waves by using two closely placed pressure sensors at one measurement site (referred to as a dual-sensor). Two typical transient incident pressure waves, a pulse wave and a step wave, are investigated in numerical simulations and laboratory experiments. Comparison of the wave separation results with their predicted counterparts shows the wave separation algorithm is successful. The results also show that the proposed wave separation technique facilitates transient-based pipeline condition assessment.

Key words | hydraulic transient, pipeline condition assessment, unsteady flow, water hammer, wave separation

He Shi (corresponding author)
Jinzhe Gong
Aaron C. Zecchin
Martin F. Lambert
Angus R. Simpson
School of Civil, Environmental and Mining Engineering,
University of Adelaide,
SA 5005, Adelaide,
Australia
E-mail: *he.shi@adelaide.edu.au*

INTRODUCTION

The aging of water distribution systems worldwide has brought many issues, ranging from significant water and energy losses (Colombo & Karney 2002) to risks to public health due to possible pathogen intrusion (Karim *et al.* 2003). Over the past two decades, hydraulic transients (water hammer waves) have been identified as a useful tool for non-invasive pipeline leak detection (Mpesha *et al.* 2001; Ferrante & Brunone 2003; Covas *et al.* 2005; Lee *et al.* 2005; Soares *et al.* 2011; Ferrante *et al.* 2013; Duan 2016), blockage detection (Sattar *et al.* 2008; Meniconi *et al.* 2013; Massari *et al.* 2014), wall condition assessment (Gong *et al.* 2013; Stephens *et al.* 2013) and general system parameter identification (Zecchin *et al.* 2013, 2014a). When undertaking a hydraulic transient analysis of a pipeline system, a transient disturbance (a pulse or a step pressure wave) is typically introduced by abruptly operating a valve. Then the transient pressure wave propagates along the pipe in both upstream and downstream directions. Any physical changes or anomalies in a pipeline will affect the propagation of transient pressure waves, resulting in specific reflections. These reflections can be analysed in either the time or frequency domain, in order to diagnose the anomalies in the pipeline system.

doi: 10.2166/hydro.2017.146

Most existing studies are based on the analysis of the transient pressure measured by a single sensor, or by multiple sensors usually separated by a significant distance along pipes. However, there are often simultaneous waves travelling in opposite directions. The hydraulic pressure at any single point in a pipeline can be expressed as the sum of a travelling pressure wave coming from upstream of the measurement point and a travelling pressure wave coming from downstream. As a consequence, for a single pressure sensor, the measured signal is always a superimposed signal of waveforms propagating upstream and downstream. One measurement strategy to avoid a superposition problem is by placing the measurement point at a dead end to ensure the reflection comes only from one direction (Gong *et al.* 2014). However, when investigating transmission mains, which may be tens of kilometres long, it is not always practical to find an ideal measurement point at a dead end. Moreover, when multiple anomalies exist on both sides of a sensor, which is the common case in most pipelines, the measured pressure signal can be very complex and difficult to interpret, even when multiple measurement sites are used (Gong *et al.* 2016a).

To investigate and extract the directional information of travelling transient pressure waves, Gong *et al.* (2012a) proposed a technique that uses two pressure sensors (100 m spaced in a pipe with an internal diameter 600 mm) to separate the pressure waves travelling downstream from those travelling upstream along a pipeline. In a subsequent study by Gong *et al.* (2012b), a new measurement strategy, which involved the use of two pressure sensors in close proximity (1 m spaced in a pipe with an internal diameter 600 mm), was proposed to facilitate the wave separation. However, these preliminary studies were limited to numerical simulations with ideal conditions where the pipeline between two sensors is assumed to be lossless and the incident wave is a sharp step signal.

Zecchin *et al.* (2014b) proposed a technique for extracting the impulse response of a single pipeline using a pair of sensors (10 m spaced in a pipe with an internal diameter of 200 mm) for measurement, and using hydraulic noise as the excitation. The hydraulic noise is in the form of wide-sense stationary pressure signals (the mean function and correlation function do not change over time). In that study, a theoretical propagation loss between two sensors was considered. However, the directional travelling waves were not extracted from the measurements. The wide-sense stationary pressure signals are difficult to achieve in practice, and only a numerical case study was conducted in that paper.

It should be noted that the use of two pressure sensors in close proximity (referred to as a 'dual-sensor' in the following) for wave separation has been studied in the acoustics research area, where acoustic waves in ducts measured by two (or more) microphones are analysed (Chung & Blaser 1980). However, hydraulic transient waves in water-filled pipes have many differences from acoustic waves propagating in the air, namely, they have a different signal bandwidth, wave magnitude and wave propagation properties where wall friction plays a much more significant role. Moreover, the research in acoustic ducts focuses on calculating the reflection and transmission coefficients, rather than splitting the directional travelling waves explicitly, which is the focus of the wave separation method developed in the current paper. In the field of pipeline transient analysis, the use of two pressure sensors in close proximity has been used for unsteady flow measurement (Washio *et al.* 1996; Kashima *et al.* 2013). However, except for the preliminary numerical work reported in Gong *et al.* (2012a, 2012b) and Zecchin *et al.* (2014b), to the knowledge of the authors, there is no study on the separation of hydraulic transient waves using a dual-sensor in pressurised pipelines.

The research reported in the current paper develops a systematic wave separation algorithm that can extract the two directional travelling hydraulic transient waves from pressure traces as measured by two closely spaced pressure sensors. Compared to the preliminary numerical work in Gong *et al.* (2012a, 2012b) and Zecchin *et al.* (2014b), the new developments include: (1) an experimental data-driven approach to estimate the transfer function between the two sensors, which enables wave separation without the knowledge of the specific pipe parameters (e.g. flow rate, friction factor, and diameter of the pipe); (2) the extraction and removal of the incident waves, making the algorithm applicable to real incident waves with curved wave fronts rather than the theoretical sharp incident waves used in previous studies; and (3) the first experimental verification of the wave separation technique.

To validate the wave separation algorithm, a pulse incident wave is used in a numerical study and a step wave is considered in a laboratory study. In both studies, as presented in this paper, the comparison between the extracted directional reflection trace with its counterpart, which has a reflection from one direction only, shows the wave separation algorithm is successful. The wave separation algorithm provides the directional information of travelling transient pressure waves in pipelines and simplifies the interpretation of the signals. The directional waves, as obtained in the laboratory study, are then used to determine the properties of two deteriorated pipe sections in the experimental system (simulated by short pipe sections with thinner wall thicknesses). The results demonstrate that the proposed wave separation technique can adequately facilitate transient-based pipeline condition assessment. Limitations of the technique and practical challenges are discussed before drawing the conclusions.

WAVE SEPARATION ALGORITHM USING A DUAL-SENSOR

Hydraulic wave propagation theory

The transient behaviour of pressurised fluid within a closed conduit pipeline system is governed by the so-called water hammer equations, which are a series of two one-dimensional (1-D) quasi-linear hyperbolic differential equations describing mass and momentum conservation (Wylie & Streeter 1993; Chaudhry 2014). The solution of the water hammer equations can be expressed in terms of pressure waves travelling upstream and downstream (Wylie & Streeter 1993; Chaudhry 2014). This is a consequence of the mathematical properties of the hyperbolic equations, but also reflects the physics of the fluid, that is, the fluid pressure at any single point in a pipeline can be expressed as the sum of a pressure wave travelling in the positive direction and a pressure wave travelling in the negative direction, i.e.:

$$p(x, t) = p^{+}(x, t) + p^{-}(x, t) \tag{1}$$

where p is the total pressure as measured by a sensor, p^{+} is the positive pressure wave coming from the upstream, p^{-} is the negative pressure wave travelling from the downstream to the upstream, x is the axial coordinate along the pipe and t is time.

Applying the Laplace transform to Equation (1) to transform the signals into the Laplace (or frequency) domain, the pressure signal is then described as:

$$P(x, s) = P^{+}(x, s) + P^{-}(x, s) \tag{2}$$

where s is the complex valued frequency (the Laplace variable), and the capital P represents pressure signals in the frequency domain.

A typical configuration for transient pressure measurement using a dual-sensor in a pipeline is given in Figure 1(a): a side discharge valve G is used as the transient generator, T_1 and T_2 are the pressure sensors, and $p_1(t)$ and $p_2(t)$ are the measured pressure traces by T_1 and T_2, respectively. The pipe section between T_1 and T_2 is assumed to act as a linear time-invariant (LTI) system (Ljung 1999), where the pressures $p_1^{+}(t)$ and $p_2^{+}(t)$ are the positive travelling

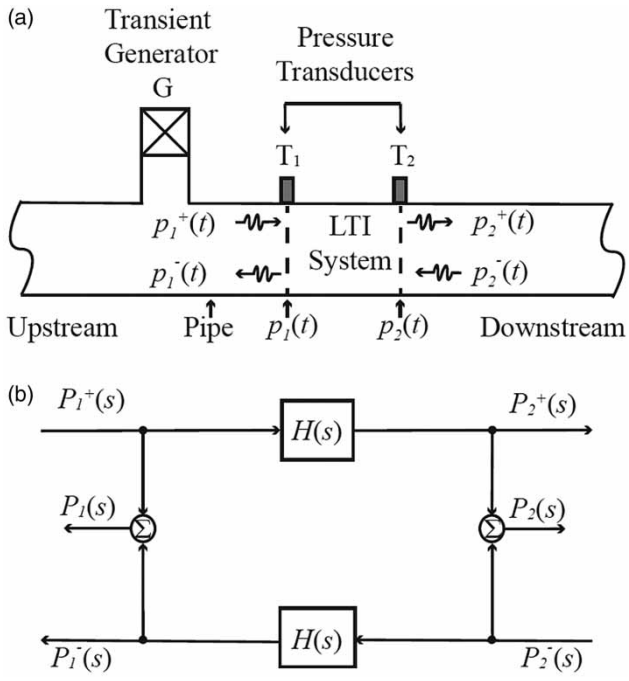

Figure 1 | (a) Proposed configuration for the pressure transient test with a dual-sensor in a pipeline; and (b) corresponding block diagram in the frequency domain illustrating the wave propagation (LTI System = Linear Time Invariant System).

waves at T_1 and T_2, respectively, and $p_1^-(t)$ and $p_2^-(t)$ are the negative travelling waves at T_1 and T_2, respectively.

The configuration can be described by a block diagram as shown in Figure 1(b). A transfer function $H(s)$ is the representation of the wave propagation dynamics between sensor T_1 and T_2, where $P_1(s)$ and $P_2(s)$ are the Laplace transforms of $p_1(t)$ and $p_2(t)$ respectively (as for all other capitalised symbols). Based on Equation (2), $P_1(s)$ and $P_2(s)$ can be written as the sum of the positive and the negative travelling waves as in Equations (3) and (4):

$$P_1(s) = P_1^+(s) + P_1^-(s) \tag{3}$$

$$P_2(s) = P_2^+(s) + P_2^-(s) \tag{4}$$

The outputs of the system [$P_1^-(s)$ and $P_2^+(s)$] and the inputs of the system [$P_2^-(s)$ and $P_1^+(s)$] are related by the transfer function $H(s)$ and written as:

$$P_1^-(s) = P_2^-(s)H(s) \tag{5}$$

$$P_2^+(s) = P_1^+(s)H(s) \tag{6}$$

Substituting Equations (5) and (6) into Equations (3) and (4), respectively, yields:

$$P_1(s) = P_1^+(s) + P_2^-(s)H(s) \tag{7}$$

$$P_2(s) = P_1^+(s)H(s) + P_2^-(s) \tag{8}$$

$P_2^-(s)$ can be eliminated by multiplying Equation (8) by $H(s)$ and then subtracting Equation (7) from the resulting equation, yielding the final result:

$$P_1^+(s) = \frac{P_1(s) - P_2(s)H(s)}{1 - H^2(s)} \tag{9}$$

Substituting Equation (9) into Equation (3) and rearranging gives:

$$P_1^-(s) = \frac{P_2(s)H(s) - P_1(s)H^2(s)}{1 - H^2(s)} \tag{10}$$

From Equations (9) and (10), the positive travelling wave $P_1^+(s)$ and negative travelling wave $P_1^-(s)$ can be extracted from the original pressure measurements [$P_1(s)$ and $P_2(s)$] using the transfer function $H(s)$ in the transform domain.

Determination of the transfer function $H(s)$

Analytic representation

The transfer function $H(s)$ is a characterisation of the physical wave propagation dynamics of the pipe section. In 1-D water hammer analysis, the transfer function $H(s)$ for the pipe between two sensors can be expressed analytically as:

$$H(s) = e^{-\Gamma(s)l} \tag{11}$$

where l is the length between two sensors, $\Gamma(s)$ is the propagation operator or propagation constant that describes the frequency dependent attenuation and phase change per unit length (Wylie & Streeter 1993). $\Gamma(s)$ can be expressed in a general form by (Zecchin 2009):

$$\Gamma(s) = \frac{1}{a}\sqrt{[s + R(s)][s + C(s)]} \tag{12}$$

where a is the wave speed, $R(s)$ and $C(s)$ represent the resistance and compliance terms, respectively.

Specific expressions of the propagation operator $\Gamma(s)$ can be derived from the general form for specific hydraulic conditions (e.g. for laminar or turbulent flow, for elastic or viscoelastic pipes) (Zecchin 2009; Gong *et al.* 2016b). If only steady friction and elastic pipe behaviour are considered, as is the case in this research, then $C(s) = 0$, and $R(s) = R$. The resistance term can be given by (Zecchin 2009):

$$R = \frac{f|\bar{Q}|}{DA} \tag{13}$$

where f is the Darcy–Weisbach friction factor, $|\bar{Q}|$ is the absolute value of the steady-state flow, D is the internal diameter of the pipe, and A is the cross-sectional area of the pipe.

From a practical perspective, using the analytic form (11), $H(s)$ can be completely specified using measured values of l, a, and a calibrated value of R (or known D with estimates of $\bar{Q}$ and f).

Experimental representation

As an alternative to the analytic expression for $H(s)$, the properties of the transfer function can also be determined experimentally. In hydraulic transient analysis, a pipeline system is typically excited by abruptly opening or closing a valve, which results in a discrete wave with a short duration as an incident pressure wave (e.g. a sharp step or pulse wave). Under these conditions, an assumption can be made that during the time of the incident wave entering into the system at T_1 then exiting the system at T_2, there are no transient waves entering the system from T_2 (i.e. $p_2^-(t) = 0$ in Figure 1). This assumption is often valid when the incident wave is short, and the system is excited from a steady state condition. Therefore, the LTI system in Figure 1(a) can be temporarily treated as a single-input and single-output system for this short time period. The input is the incident wave $p_1^+(t) = p_{1i}(t)$ at T_1, and the output is the incident wave $p_2^+(t) = p_{2i}(t)$ at T_2. The incident waves $p_{1i}(t)$ and $p_{2i}(t)$ can be extracted from the original measured pressure trace $p_1(t)$ and $p_2(t)$ by applying a rectangular time window (i.e. truncating the short signal section that includes the wave front out of the whole pressure trace).

The transfer function $H(s)$ is the linear mapping from an input to an output in the Laplace domain, and can be given by:

$$H(s) = \frac{P_{2i}(s)}{P_{1i}(s)} \tag{14}$$

where $P_{1i}(s)$ and $P_{2i}(s)$ are the Laplace transforms of the incident waves at T_1 and T_2, respectively. Note that the experimental approach does not require any flow rate information except that there is no wave (or relatively very small wave) in one direction, which is an advantage over the analytical approach.

The wave separation algorithm

In Figure 1(a), when an incident pressure wave is generated at G and arrives at sensor T_1, the positive travelling pressure wave at T_1 contains the incident wave and the reflected wave coming from upstream of T_1. The reflected wave is the focus because it carries the pipeline information that can be used for pipeline condition assessment. However, compared to the incident wave, the reflections due to wall deterioration are usually small (Gong *et al.* 2015). Given this, removing the dependence of the incident wave from the wave separation results leads to clearer separated directional travelling waves, and the method is described below.

In Figure 1(a), the positive travelling waves can be written as the sum of the incident wave and the reflected wave coming from upstream:

$$p_1^+(t) = p_{1i}(t) + p_{1r}^+(t) \tag{15}$$

$$p_2^+(t) = p_{2i}(t) + p_{2r}^+(t) \tag{16}$$

where $p_{1r}^+(t)$ and $p_{2r}^+(t)$ are the reflected waves coming from upstream of the measurement points T_1 and T_2 respectively. The negative travelling waves $p_1^-(t)$ and $p_2^-(t)$ can be written as the negative travelling reflected waves $p_{1r}^-(t)$ and $p_{2r}^-(t)$:

$$p_1^-(t) = p_{1r}^-(t) \tag{17}$$

$$p_2^-(t) = p_{2r}^-(t) \tag{18}$$

As a result, the pressure waves as measured by the sensors at points T_1 and T_2 can be described by:

$$p_1(t) = p_{1i}(t) + p_{1r}(t) \tag{19}$$

$$p_2(t) = p_{2i}(t) + p_{2r}(t) \tag{20}$$

where $p_{1r}(t) = p_{1r}^+(t) + p_{1r}^-(t)$ and $p_{2r}(t) = p_{2r}^+(t) + p_{2r}^-(t)$. As a sharp step or pulse wave is usually used as an incident wave, and in the time domain the incident waves $p_{1i}(t)$ and $p_{2i}(t)$ can be easily identified and extracted from the measured pressure traces using a time-windowing procedure as for Equation (14). Similarly the reflections $p_{1r}(t)$ and $p_{2r}(t)$ can also be extracted by applying an appropriate rectangular time window.

Transforming Equations (15)–(20), and then substituting the transformed equations and Equation (14) into Equations (9) and (10), rearrangement of the final result yields the

following wave forms for the two reflected wave components:

$$P_{1r}^{+}(s) = \frac{P_{1r}(s) - P_{2r}(s)H(s)}{1 - H^2(s)} \tag{21}$$

$$P_{1r}^{-}(s) = \frac{P_{2r}(s)H(s) - P_{1r}(s)H^2(s)}{1 - H^2(s)} \tag{22}$$

The inverse Laplace transforms of Equations (21) and (22) will give the positive travelling reflected waves and the negative travelling reflected waves in the time domain.

For analysis of real pipeline systems where the pressure signals measured by sensors are used, the value of the Laplace variable is restricted to the imaginary axis, i.e. $s = i\omega$, where i is the imaginary unit and ω is the radial frequency. Consequently, the Fourier transform can be used instead of the Laplace transform.

To apply the wave separation algorithm to pressure traces [$p_1(t)$ and $p_2(t)$] measured by a dual-sensor as in Figure 1(a), the following steps will be performed:

1. Time-windowing to separate incident waves and reflections in the original pressure traces measured by a dual-sensor using Equations (19) and (20).
2. Transfer incident waves and reflections into the frequency domain by using the Fourier transform.
3. Determine the transfer function between two sensors using the analytic Equation (11) or using the experimental Equation (14).
4. Extract the directional reflection waves in the frequency domain using Equations (21) and (22).
5. Transfer wave separation results into the time domain using an Inverse Fourier Transform, or using the results directly in the frequency domain for further analysis, e.g. determine the frequency response of the pipe section.

It should be noted that, when other incident waves are used in place of discrete waves with a short duration, Step 1 can be ignored and Equations (9) and (10) in Step 4 used instead. Before the wave separation algorithm is applied to real data, pre-processing may be needed, including determining the effective frequency range to minimise the impact of high frequency noise on the time domain reconstruction of the separated reflected waves. Because the analysis is built on linear systems theory, the incident waves should be small perturbations to limit the effect of linearization (Lee & Vítkovský 2010).

NUMERICAL VERIFICATION

To verify the dual-sensor wave separation algorithm, numerical simulations have been conducted. A single pulse hydraulic pressure wave is used as the incident wave in the numerical investigations since it has never been studied previously for wave separation.

System layout and procedure

For the numerical study, a metallic pipeline system with two short deteriorated sections and one relatively long section with a change of pipe class is considered. The layout of the numerical pipeline system is given in Figure 2. The physical details of the pipe sections are summarised in Table 1. The length of each reach is carefully designed to satisfy the Courant condition for method of characteristics (MOC) simulations (with a time step of 0.05 ms). The system is a reservoir-pipeline-reservoir (R-P-R) system. Reservoir 1 has a constant head of 60 m, and the constant head for Reservoir 2 is 57 m. The total length of the pipeline is 1 km. The steady-state flow is calculated as 0.264 m^3/s, corresponding to a velocity of 1.34 m/s. For the normal pipe sections, the internal diameter is 500 mm, the wall thickness is 8 mm, the Reynolds number is 4.75×10^5 (indicating turbulent flow) and the wave speed is 1,154 m/s. Two pipe sections L_2 and L_9 which have thinner wall thicknesses (6 and 5 mm), larger internal pipe diameters (504 and 506 mm) and smaller wave speeds (1,083 and 1,036 m/s) are placed in the system to simulate the deteriorated sections (e.g. extended internal corrosion). Pipe section L_7 with a length of approximately 150 m, the same internal diameter as the majority of the pipe, but a thinner wall thickness (7 mm) and thus a lower wave speed (1,123 m/s), is placed in the system to simulate a section of a lesser pipe class. A significantly higher Darcy–Weisbach friction factor (0.03) has been assigned to sections L_2 and L_9 to represent the effect of a much higher wall surface roughness as

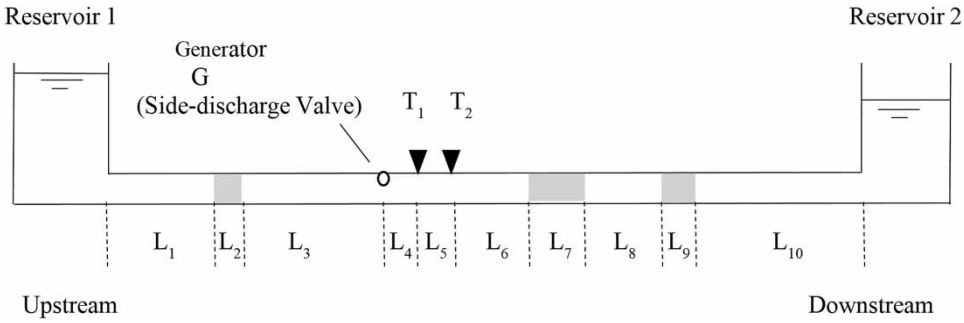

Figure 2 | Layout of the pipeline system used in the numerical simulations (not to scale). See Table 1 for physical details.

would result from a pipe that has experienced corrosion. The dual sensor (with a sensor spacing of 0.9809 m) is placed in the middle of the pipeline system at T_1 and T_2, respectively. A side-discharge valve which is located at 0.9809 m upstream from T_1 is used as the transient generator. The steady-state discharge through the side-discharge valve is set as 0.01 m^3/s. The length of each pipe section has been selected to satisfy the Courant condition for the time domain MOC simulations so that no interpolation scheme is required (Chaudhry 2014).

An incident pressure wave is generated at time $t = 0.1$ s by manoeuvring the side-discharge valve. The incident wave is a pulse wave with 20 ms duration, generated by fully closing the side discharge valve then fully opening it again (the manoeuvre is designed numerically that the incident pulse pressure wave as generated has a shape similar to a cosine function changing from $-\pi$ to π, to make the signal more realistic than a sharp instantaneous rise). The response of the pipeline system is simulated by MOC with steady friction only.

Table 1 | Physical details of the pipe sections used in the numerical simulations

Link	Length (m)	Internal diameter (mm)	Wall thickness (mm)	Wave speed (m/s)	Friction factor (–)
L1	415.9593	500	8	1,154	0.017
L2	12.0213	504	6	1,083	0.030
L3	72.0096	500	8	1,154	0.017
L4	0.9809	500	8	1,154	0.017
L5	0.9809	500	8	1,154	0.017
L6	69.9901	500	8	1,154	0.017
L7	150.1451	500	7	1,123	0.017
L8	60.0080	500	8	1,154	0.017
L9	11.9944	506	5	1,036	0.030
L10	205.9890	500	8	1,154	0.017

Wave separation results

The pressure traces at T_1 and T_2 are used as the measurements $p_1(t)$ and $p_2(t)$, which are shown in Figure 3(a). The wave separation algorithm is applied to the measurements

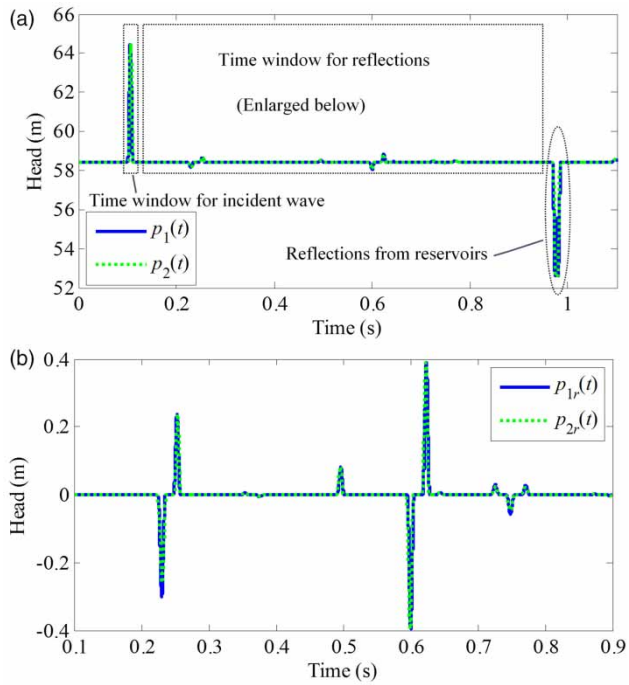

Figure 3 | (a) Numerical pressure traces measured at T_1 and T_2; and (b) enlarged view of the wave reflections from deteriorated sections in the numerical study.

$p_1(t)$ and $p_2(t)$ by following the steps which were outlined previously. The reflected waves $p_{1r}(t)$ and $p_{2r}(t)$ are shown in Figure 3(b). It can be seen from Figure 3(b) that the pressure reflections as recorded by the dual-sensor possess a complex form of pressure wave fluctuations, although only three uniform sections with lower wave speeds are considered. This complexity is due to the superimposition of the reflections from the three thinner-walled sections.

Figure 4(a) shows the reflections from upstream of T_1 and Figure 4(b) gives the reflections from downstream. The pressure waves $p^+_{1r\_A}(t)$ and $p^-_{1r\_A}(t)$ are obtained by using the analytic expression of the transfer function between two sensors according to Equations (11) and (12), while $p^+_{1r\_E}(t)$ and $p^-_{1r\_E}(t)$ are calculated from the experimental transfer function which is estimated by using the extracted incident waves according to Equation (14). The analytically and experimentally determined transfer functions are consistent within the bandwidth of the incident wave.

For a comprehensive comparison, the wave separation results are compared with predicted results as computed directly from the MOC. The predicted results for upstream reflections ($p^+_{1r\_P}(t)$ as shown in Figure 4(a)) are obtained from MOC modelling the system similar to that depicted in Figure 2, but only with one deteriorated section L_2 existing on the upstream side of the sensors. On the downstream side of the sensors, there are just uniform intact pipes (i.e. L_7 and L_9 are set as the same as the intact sections). Hence, the simulated reflections only come from upstream and are a result of section L_2. Similarly, the predicted results for downstream reflections ($p^-_{1r\_p}(t)$ as shown in Figure 4(b)) are acquired by MOC modelling with no defective sections existing on the upstream side of the sensors, so reflections only occur on the downstream side of the sensors and include reflections from sections L_7 and L_9.

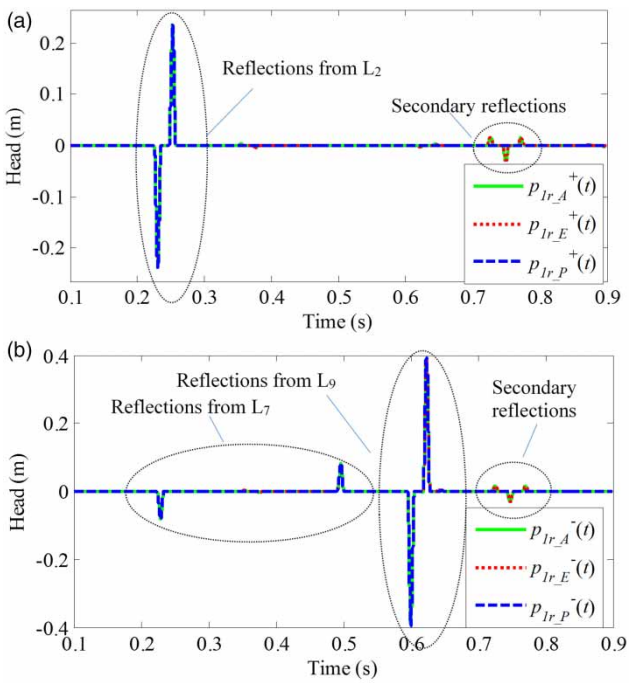

Figure 4 | (a) Directional reflected pressure waves travelling from upstream to downstream; and (b) directional reflected pressure waves travelling from downstream to upstream.

It can be seen in Figure 4 that the reflections from the three thinner-walled pipe sections are separated and clearly shown in the directional waves $p^+_{1r}(t)$ and $p^-_{1r}(t)$ respectively. The separation results from two different transfer function calculation methods (analytical and experimental) are almost identical, and both of them have an excellent match with the MOC predictions. It should be noted that the separated results of directional waves include multiple reflections while the predicted results do not. The multiple reflections are due to secondary reflections between anomalous sections on the two sides of sensors. For example, when all three thinner-walled sections are considered in the simulation, the major wave reflections from sections L_7 and L_9 (as shown in Figure 4(b)) will propagate from downstream to upstream, pass the dual-sensor and then be reflected by section L_2 as secondary reflections. These secondary reflections will then propagate downstream as part of $p^+_{1r}(t)$. Nevertheless, the numerical simulation demonstrates that the proposed wave separation approach is valid for pipelines excited by single pulse incident pressure waves.

EXPERIMENTAL VERIFICATION

Laboratory experiments have been conducted in a single copper pipeline in the Robin Hydraulics Laboratory at the University of Adelaide. The laboratory system is a copper pipe (internal diameter 22.14 mm, total length 37.43 m) bounded by two pressurised tanks. The pressurised tanks can be isolated by an in-line valve to make the system a

reservoir-pipeline-valve (R-P-V) configuration. A step incident pressure wave is used to avoid repetition from the numerical study and it better represents the incident waves used in the field.

System layout and procedure

The layout of the pipeline system used in the experiments is shown in Figure 5 and the physical details are given in Table 2. The wave speeds are calculated using the theoretical wave speed formula (Wylie & Streeter 1993). The following parameter values are used: Young's modulus of a copper pipe $E = 124.1\,\text{GPa}$, restraint factor for thick-walled copper pipe anchored throughout $c_1 = 1.006$, bulk modulus of elasticity of water at 15 °C is $K = 2.419\,\text{GPa}$, and density of water at 15 °C is $\rho = 999.1\,\text{kg/m}^3$. The restraint factor is a dimensionless parameter that depends on the elastic properties and the constraint condition of the pipe (Wylie & Streeter 1993).

The majority of the pipeline is in Class A. Two short pipe sections of Class B and C, respectively, which have thinner wall thicknesses than that of Class A, are placed in the system to simulate pipe sections with wall deterioration. The head in the pressurised tank was controlled at approximately 31 m during the experiments. The in-line valve at the other end was kept closed during the experiments.

A solenoid side-discharge valve was used as the transient generator (G) and placed at the same location as pressure sensor T_1. The other pressure sensor (T_2) was located upstream (on the left) of the transient generator separated by a distance of 0.99 m. A step pressure wave was generated by abruptly closing the solenoid valve in approximately 3 ms. The pressure responses were measured by the two sensors with a sampling frequency of 20 kHz.

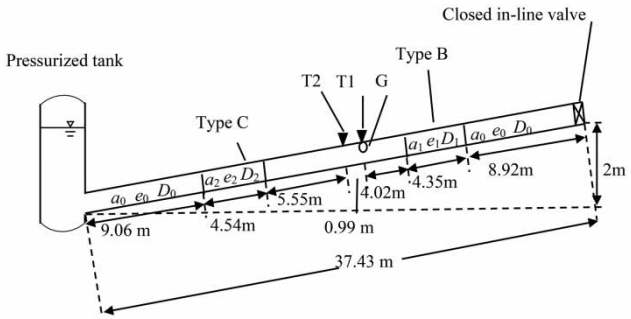

Figure 5 | System layout of the experimental pipeline system.

Table 2 | Physical details of the pipeline system used in the laboratory experiments

Pipe class	Internal diameter (symbol = value (mm))	Wall thickness (symbol = value (mm))	Wave speed (symbol = value (m/s))
A	$D_0 = 22.14$	$e_0 = 1.63$	$a_0 = 1{,}319$
B	$D_1 = 22.96$	$e_1 = 1.22$	$a_1 = 1{,}273$
C	$D_2 = 23.58$	$e_2 = 0.91$	$a_2 = 1{,}217$

Wave separation results

The original head responses as measured by the dual-sensor are shown in Figure 6(a). The pressure oscillations before the first boundary reflection are the focus and shown in Figure 6(b). The steady-state head is determined by averaging a period of measurement before the incident wave and then subtracting from the raw measurements. The start time of the incident wave is set to zero, and the

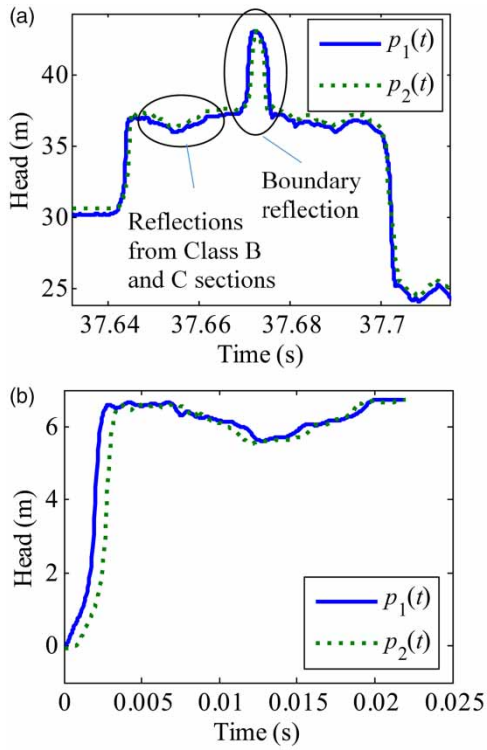

Figure 6 | (a) Original pressure traces measured in the laboratory experiments; and (b) pressure oscillations before the first boundary reflection.

pressure traces are truncated before the boundary reflections (the reflection from the tank and the closed in-line valve). It can be seen that the reflections from the Class B and Class C pipe sections are superimposed in the two measured traces, resulting in complex reflections that are difficult to interpret.

The incident waves and the wave reflections are then extracted as outlined previously in Step 1 in the analysis methodology. The measured incident waves are used to determine the experimental transfer function $H(s)$ using Equation (14) in Step 3. The amplitude spectrums of the measured wave reflections are checked to investigate the effective frequency range (the bandwidth) as depicted in Figure 7. It is found that most energy of the reflected signals is in frequencies less than 300 Hz, which represents the useful bandwidth of the pressure waves. Given this, an upper frequency bound of 600 Hz was adopted to avoid effects of noise in the high frequency range and also to cover the effective bandwidth of the reflected waves.

The positive and negative travelling pressure reflection waves $p_{1r}^{+}(t)$ (propagating towards the closed in-line valve) and $p_{1r}^{-}(t)$ (propagating towards the tank) are determined by Equations (21) and (22) for frequencies up to 600 Hz in Step 4. The results are given in Figure 8 and compared with the predicted results generated by MOC simulations (the procedure is the same as that used in the numerical study, i.e. only deterioration on one side is considered when generating the predicted results). The steady-state pressure in the MOC model is set equal to the measured steady-state pressure in the laboratory. The step incident wave in the MOC model is designed according to the measured incident step wave with a rise time of 3 ms and a pressure head magnitude of 6.60 m. The shape of a cosine function changing from π to 2π is adopted to simulate the curved wave front.

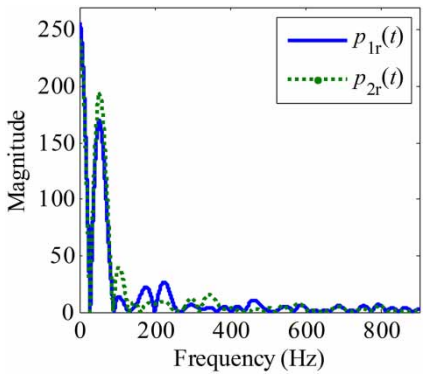

Figure 7 | Amplitude spectrum of the reflected waves.

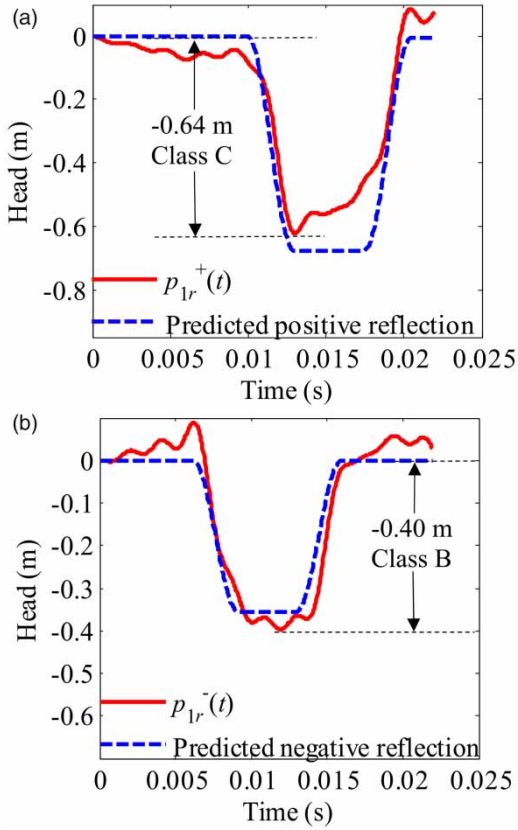

Figure 8 | (a) Directional reflected pressure waves travelling towards the closed in-line valve; and (b) directional reflected pressure waves travelling towards the tank.

It can be seen that in the directional waves, reflections from the two thinner-walled sections are separated, and the determined directional wave reflections are consistent with the numerically generated predicted results. The superimposed reflection is reconstructed by adding $p_A^{+}(t)$ and $p_A^{-}(t)$ together and then comparing them with the original measured wave reflection $p_{1r}(t)$ in Figure 9. The reconstructed reflection trace is generally consistent with the original measured reflection trace, with small differences due to the exclusion of the frequency components above 600 Hz in the wave separation. Overall, the experimental results have illustrated the feasibility of the separation of directional travelling pressure waves in pipelines using a dual-sensor.

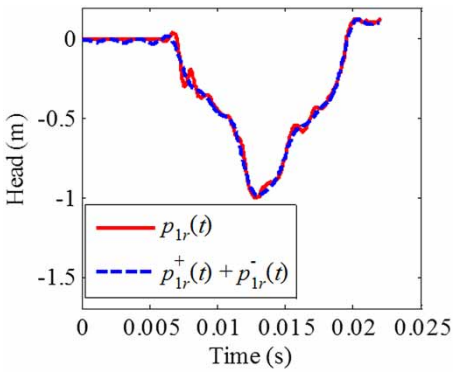

Figure 9 | Comparison between the original wave reflections measured at T_1 (the solid line) and the superimposed result of the determined directional wave reflections (the dashed line).

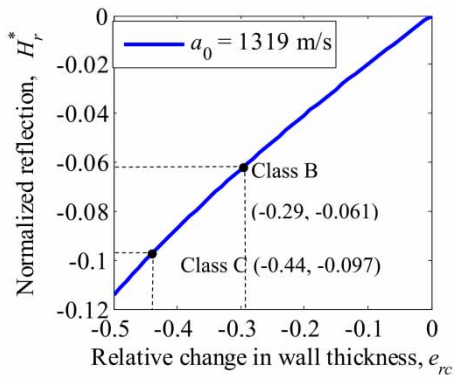

Figure 10 | Relationship between the normalized wave reflection (p_n) and the relative change in the wall thickness (e_{rc}) for the experimental pipeline.

Application to pipeline condition assessment

The time domain condition assessment technique as outlined in Gong *et al.* (2013) is now applied to the resultant directional reflection waves [$p^{+}_{1r}(t)$ and $p^{-}_{1r}(t)$ as shown in Figure 8] to determine the wall thickness of the thinner-walled sections (the Class B and C sections). It is known that the external diameter of the experimental pipeline is uniform and the change in class affects the internal diameter. For this scenario, the relationship between the relative size of a wave reflection and the relative change in the wall thickness is derived as:

$$p_n = \frac{\sqrt{\frac{(K/\rho)(1+e_{rc})}{K/\rho + e_{rc}a_0^2}} - \left[1 - 2e_{rc}\frac{(K/E)a_0^2c_1}{K/\rho - a_0^2}\right]^2}{\sqrt{\frac{(K/\rho)(1+e_{rc})}{K/\rho + e_{rc}a_0^2}} + \left[1 - 2e_{rc}\frac{(K/E)a_0^2c_1}{K/\rho - a_0^2}\right]^2} \tag{23}$$

where p_n represents the normalized head perturbation of the reflected wave and is defined as $p_n = (p_r - p_i)/p_i$, where p_r and p_i are the sizes of reflected wave and incident wave respectively; e_{rc} is the relative change in wall thickness and is defined as $e_{rc} = (e_d - e_0)/e_0$, where e_0 and e_d represent the wall thickness in the intact and deteriorated section respectively; a_0 is the wave speed in the intact pipe. Note that Equation (23) is derived under an assumption for lossless elastic pipelines.

The plot of Equation (23) is given in Figure 10. The theoretical wave speed in the intact (Class A) pipe is considered, which is $a_0 = 1319\,\text{m/s}$ as in Table 2. The range of e_{rc} used is from $e_{rc} = -0.5$ to $e_{rc} = 0$, which represents wall thickness variation from half the original wall thickness to the original wall thickness. The plot can serve as a look-up chart for condition assessment for pipes with internal changes in wall thickness.

It is obvious that the original pressure measurements as shown in Figure 9 cannot be directly used for condition assessment because the reflections from the Class B and the Class C sections are superimposed. In contrast, the separated directional wave reflections as shown in Figure 8 show the wave reflections from the two sections separately and clearly, and they can easily be used for further analysis.

The values of the relative wave reflections ($p_r - p_i$) from the Class C and Class B sections are determined from the minima of $p^{+}_{1r}(t)$ and $p^{-}_{1r}(t)$ respectively as shown in Figure 8, for which the results are $p^{-}_{1r} - p_i = -0.64$ m and $p^{-}_{1r} - p_i = -0.40$ m respectively. The magnitude of the incident step wave is determined as $p_i = 6.60$ m from the measured trace shown in Figure 6(b). As a result, the normalized reflections for the Class C and Class B sections are $p^{+}_n = -0.097$ and $p^{-}_n = -0.061$, respectively. Referring to the look-up chart in Figure 10, the relative change in wall thickness corresponding to these two wave reflections are $e^{+}_{rc} = -0.44$ and $e^{-}_{rc} = -0.29$, respectively. Finally, using the wall thickness of the Class A pipe of $e_0 = 1.63$ mm, the wall thicknesses in the Class C and Class B sections are determined by the reflection analysis as $e^{+} = 0.91$ mm and $e^{-} = 1.16$ mm, respectively. Compared with the wall thicknesses as given by the manufacturer ($e_2 = 0.92$ mm and

$e_1 = 1.22$ mm as shown in Table 2), the wall thicknesses are estimated with relatively high accuracy.

These results have demonstrated that the wave separation algorithm as developed in this research can significantly facilitate pipeline condition assessment by resolving the complexity due to wave superposition.

DISCUSSION

Some practical issues related to real applications of transient-based pipeline condition assessment are discussed in this section. Recommended future work is also presented.

Detection resolution

The spatial resolution of detection is limited by the effective bandwidth of the pressure waves, which is itself related to the sharpness of the wave front. For a ramp incident wave, theoretically one can accurately diagnose deteriorated sections only with a length longer than $T_i a_d/2$, where T_i is the rise time of the ramp wave front and a_d is the wave speed in the deteriorated pipe section (Gong *et al.* 2013). Sections shorter than that may still be detectable but will not give a full-sized reflection, therefore the change in wall thickness will be underestimated. In the experimental study, the rise time of the incident step was about 3 ms. Using a wave speed of 1,300 m/s, the threshold is calculated as approximately 2 m.

Detection range

The length of pipe that can be assessed reliably mainly depends on the signal-to-noise ratio (SNR). It is expected that measurements in the field can have stronger noise than in the laboratory (e.g. due to pump operations). The frequency range to include in the analysis should be selected carefully to balance the SNR and detection resolution (as discussed above). Usually low frequency waves have better SNR than high frequency components, because the latter typically have less initial energy and suffer higher damping rates. A spectrum analysis for the wave reflections (as described in the Experimental verification section) will help to determine the useful bandwidth. Nevertheless, field trials by the authors confirmed that a step transient pressure wave can travel many kilometres with insignificant attenuation in water transmission mains (diameter 600 mm) (Stephens *et al.* 2013; Gong *et al.* 2015, 2016a). However, the sharpness of the wave front decreases over the distance of propagation.

Non-uniform deterioration

In real pipelines, deteriorated sections most likely have non-uniform wall thickness variations. As a result, the wave reflections may not have sharp edges as shown in the laboratory study. In such cases, the extrema of the reflections should be used to calculate the normalized head perturbation. The determined wall thickness represents the general condition of the deteriorated section.

Other sources of reflections

In addition to deteriorated pipe sections, wave reflections can be induced by other sources, which typically include changes in pipe material and class, leaks, blocks, branches and air pockets. Priori information of pipeline systems (e.g. as constructed drawings) will be helpful in identifying the source of wave reflections. The characteristics of the wave form can also facilitate the categorisation (e.g. discrete blocks introduce extended positive reflections while leaks introduce extended negative reflections). Note that pipe joints typically do not introduce noticeable reflections, since the dimension of joints is much smaller than the effective wavelength.

Accuracy of transfer function

A topic for future work is to enhance the accuracy in the determination of the transfer function between the two pressure sensors. Error in the transfer function will affect the wave separation and therefore the condition assessment. It can be induced by background noise and the inconsistency among pressure transducers (i.e. for the same pressure condition, different sensors may give slightly different readings). The use of sensor arrays to provide redundant information may be helpful in enhancing the accuracy.

CONCLUSIONS

A wave separation algorithm has been developed for extracting the directional hydraulic transient pressure waves that travel along a pipeline in the downstream and upstream directions, respectively. Discrete incident transient waves, such as a single pulse or a step wave which are commonly used in transient-based pipeline fault detection, are used to excite a pipeline system and induce reflections from deteriorated pipe sections. The wave separation is achieved by analysing the pressure responses of the pipeline as measured by a proximity dual-sensor setup. The wave separation resolves the complexity of the superposition of travelling pressure waves in a pipeline, providing directional information of wave reflections and simplifying the wave forms. The key contributions of the research include: (1) the development of an experimental technique for estimating the transfer function between two sensors that is more practical than analytical estimation for real pipelines with parameter uncertainties; (2) the further development of the wave separation algorithm to enhance the accuracy for the separation of the relatively small wave reflections by removing the dependence of the relatively large incident wave; and (3) the verification of the wave separation technique by numerical and laboratory experiments.

In the numerical simulations, a discrete pulse pressure wave is considered as the incident wave, which has not been studied previously for hydraulic transient wave separation in pipelines. Three thinner-walled pipe sections are placed in the numerical pipeline system, with two of them simulating deteriorated sections due to internal corrosion and one simulating a section with a lower pipe class. The wave separation algorithm has been successfully implemented, with the resultant directional reflection waves consistent with the predicted results.

Experimental verification of the hydraulic transient wave separation algorithm has been conducted. A step transient pressure wave generated by a fast closure of a side-discharge valve is considered as the incident wave. The original pressure responses as measured by the dual-sensor spaced at 0.99 m include the superimposed wave reflections from two thinner-walled pipe sections. The directional reflection waves are extracted by the wave separation algorithm and the results are generally consistent with the numerically generated predicted results. An existing pipeline condition assessment technique that is based on direct time domain analysis of wave reflections is adopted and applied to the extracted directional waves. The wall thicknesses of the two thinner-walled pipe sections are estimated from the reflected waves by using the pipe wall thickness change look-up chart and the results are consistent with the specifications provided by the manufacturer. The experimental study has validated the proposed wave separation algorithm, and confirmed the usefulness of the algorithm in transient-based pipeline condition assessment and fault detection.

ACKNOWLEDGEMENTS

The research presented in this paper has been supported by the Australia Research Council through the Discovery Project Grant DP140100994 and the Linkage Project Grant LP130100567.

REFERENCES

Chaudhry, M. H. 2014 *Applied Hydraulic Transients*. Springer, New York, NY.

Chung, J. Y. & Blaser, D. A. 1980 Transfer function method of measuring induct acoustic properties. I. Theory. *J. Acoust. Soc. Am.* **68** (3), 907–913.

Colombo, A. F. & Karney, B. W. 2002 Energy and costs of leaky pipes toward comprehensive picture. *J. Water Resour. Plann. Manage.* **128** (6), 441–450.

Covas, D., Ramos, H. & De Almeida, A. B. 2005 Standing wave difference method for leak detection in pipeline systems. *J. Hydraul. Eng.* **131** (12), 1106–1116.

Duan, H.-F. 2016 Transient frequency response based leak detection in water supply pipeline systems with branched and looped junctions. *J. Hydroinform.* **19** (1), 17–30.

Ferrante, M. & Brunone, B. 2003 Pipe system diagnosis and leak detection by unsteady-state tests. 1. Harmonic analysis. *Adv. Water Resour.* **26** (1), 95–105.

Ferrante, M., Massari, C., Todini, E., Brunone, B. & Meniconi, S. 2013 Experimental investigation of leak hydraulics. *J. Hydroinform.* **15** (3), 666–675.

Gong, J., Zecchin, A. C., Lambert, M. F. & Simpson, A. R. 2012a Signal separation for transient wave reflections in single pipelines using inverse filters. In: *World Environmental and Water Resources Congress 2012: Crossing Boundaries, ASCE*, Albuquerque, New Mexico, USA, pp. 3275–3284.

Gong, J., Lambert, M. F., Simpson, A. R. & Zecchin, A. C. 2012b Distributed deterioration detection in single pipelines using transient measurements from pressure transducer pairs. In: *11th International Conference on Pressure Surges* (S. Anderson, ed.). BHR Group, Lisbon, Portugal, pp. 127–140.

Gong, J., Simpson, A. R., Lambert, M. F., Zecchin, A. C., Kim, Y. & Tijsseling, A. S. 2013 Detection of distributed deterioration in single pipes using transient reflections. *J. Pipeline Syst. Eng. Pract.* **4** (1), 32–40.

Gong, J., Lambert, M. F., Simpson, A. R. & Zecchin, A. C. 2014 Detection of localized deterioration distributed along single pipelines by reconstructive MOC analysis. *J. Hydraul. Eng.* **140** (2), 190–198.

Gong, J., Stephens, M. L., Arbon, N. S., Zecchin, A. C., Lambert, M. F. & Simpson, A. R. 2015 On-site non-invasive condition assessment for cement mortar-lined metallic pipelines by time-domain fluid transient analysis. *Struct. Health Monit.* **14** (5), 426–438.

Gong, J., Lambert, M. F., Zecchin, A. C., Simpson, A. R., Arbon, N. S. & Kim, Y.-I. 2016a Field study on non-invasive and non-destructive condition assessment for asbestos cement pipelines by time-domain fluid transient analysis. *Struct. Health Monit.* **15** (1), 113–124.

Gong, J., Zecchin, A. C., Lambert, M. F. & Simpson, A. R. 2016b Determination of the creep function of viscoelastic pipelines using system resonant frequencies with hydraulic transient analysis. *J. Hydraul. Eng.* **142** (9), 04016023.

Karim, M. R., Abbaszadegan, M. & Lechevallier, M. 2003 Potential for pathogen intrusion during pressure transients. *J. Am. Water Works Assoc.* **95** (5), 134–146.

Kashima, A., Lee, P. J., Ghidaoui, M. S. & Davidson, M. 2013 Experimental verification of the kinetic differential pressure method for flow measurements. *J. Hydraul. Res.* **51** (6), 634–644.

Lee, P. J. & Vítkovský, J. P. 2010 Quantifying linearization error when modeling fluid pipeline transients using the frequency response method. *J. Hydraul. Eng.* **136** (10), 831–836.

Lee, P. J., Vítkovský, J. P., Lambert, M. F., Simpson, A. R. & Liggett, J. A. 2005 Frequency domain analysis for detecting pipeline leaks. *J. Hydraul. Eng.* **131** (7), 596–604.

Ljung, L. 1999 *System Identification – Theory for the User.* Prentice-Hall, Inc., Upper Saddle River, New Jersey.

Massari, C., Yeh, T. C. J., Ferrante, M., Brunone, B. & Meniconi, S. 2014 Detection and sizing of extended partial blockages in pipelines by means of a stochastic successive linear estimator. *J. Hydroinform.* **16** (2), 248–258, 10.2166/hydro.2013.172.

Meniconi, S., Duan, H. F., Lee, P. J., Brunone, B., Ghidaoui, M. S. & Ferrante, M. 2013 Experimental investigation of coupled frequency and time-domain transient test-based techniques for partial blockage detection in pipelines. *J. Hydraul. Eng.* **139** (10), 1033–1044.

Mpesha, W., Gassman, S. L. & Chaudhry, M. H. 2001 Leak detection in pipes by frequency response method. *J. Hydraul. Eng.* **127** (2), 134–147.

Sattar, A. M., Chaudhry, M. H. & Kassem, A. A. 2008 Partial blockage detection in pipelines by frequency response method. *J. Hydraul. Eng.* **134** (1), 76–89.

Soares, A. K., Covas, D. I. C. & Reis, L. F. R. 2011 Leak detection by inverse transient analysis in an experimental PVC pipe system. *J. Hydroinform.* **13** (2), 153–166.

Stephens, M. L., Lambert, M. F. & Simpson, A. R. 2013 Determining the internal wall condition of a water pipeline in the field using an inverse transient model. *J. Hydraul. Eng.* **139** (3), 310–124.

Washio, S., Takahashi, S. & Yamaguchi, S. 1996 Measurement of transiently changing flow rates in oil hydraulic column separation. *JSME Int. J. B Fluids Therm. Eng.* **39** (1), 51–56.

Wylie, E. B. & Streeter, V. L. 1993 *Fluid Transients in Systems.* Prentice Hall Inc., Englewood Cliffs, New Jersey, USA.

Zecchin, A. C. 2009 *Laplace-domain Analysis of Fluid Line Networks with Application to Time-Domain Simulation and System Parameter Identification*. PhD Dissertation, School of Civil, Environmental and Mining Engineering, The University of Adelaide, Adelaide.

Zecchin, A. C., White, L. B., Lambert, M. F. & Simpson, A. R. 2013 Parameter identification of fluid line networks by frequency-domain maximum likelihood estimation. *Mech. Syst. Signal Process.* **37** (1–2), 370–387.

Zecchin, A., Lambert, M., Simpson, A. & White, L. 2014a Parameter identification in pipeline networks: transient-based expectation-maximization approach for systems containing unknown boundary conditions. *J. Hydraul. Eng.* **140** (6), 04014020.

Zecchin, A. C., Gong, J., Simpson, A. R. & Lambert, M. F. 2014b Condition assessment in hydraulically noisy pipeline systems using a pressure wave splitting method. *Proc. Eng.* **89**, 1336–1342.

First received 1 December 2016; accepted in revised form 12 May 2017. Available online 18 July 2017